FIRST STREET FOUNDATION

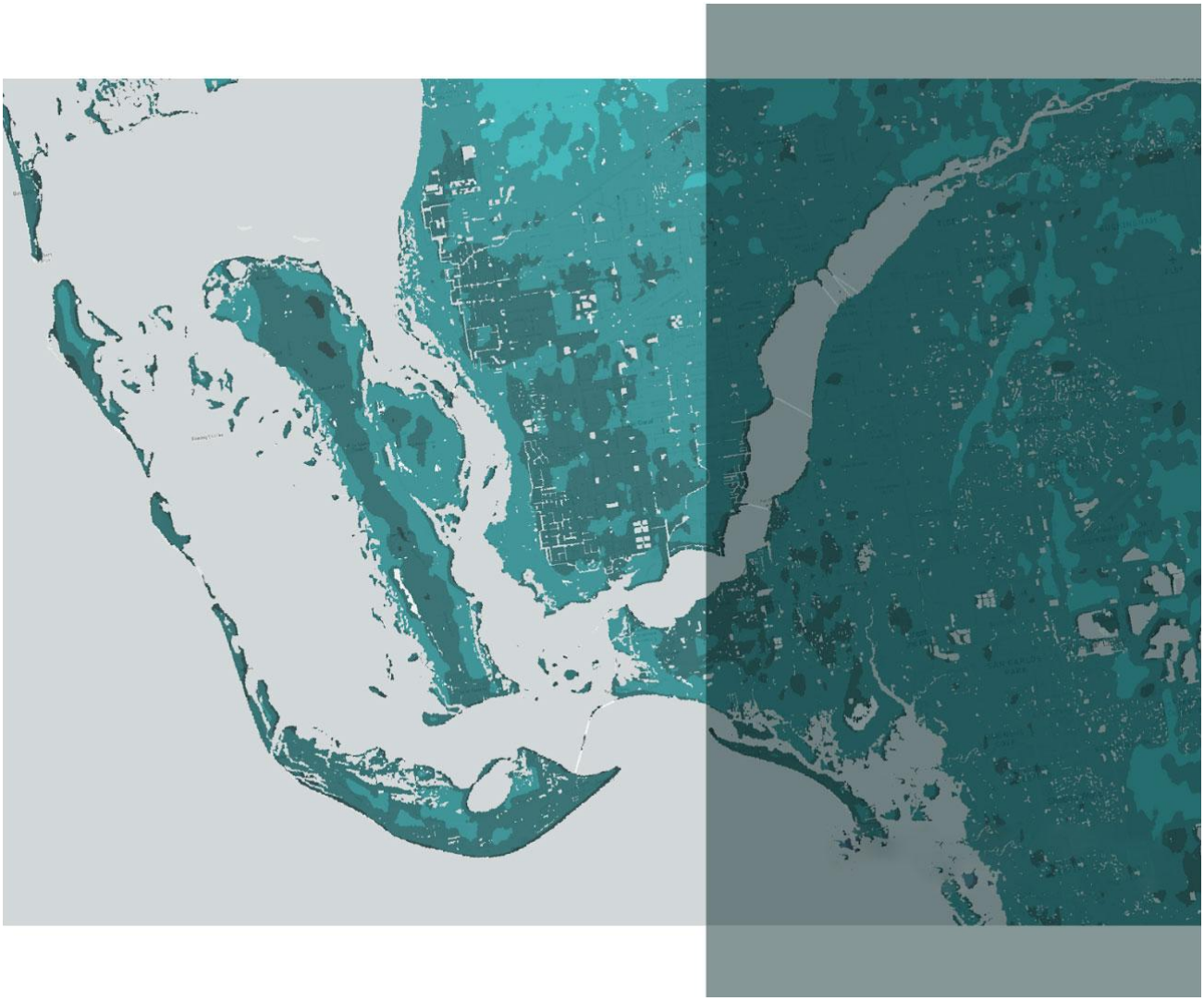

First Street Foundation - Wind Model

Technical Methodology Document

February 27th, 2023

Table of Contents:

EXECUTIVE SUMMARY **3**

DATA SOURCES & TERMINOLOGY **4**

Table 1: Data Sources 4

WIND HAZARD METHODOLOGY **5**

2.1 Hurricane Tracks 5

Figure 1: Sample of 50 hurricane tracks from the CESM2 Global Climate Model for the current time period (2015-2030). 6

2.2 Wind Field Modeling 6

2.2.1 Wind hazard statistics 7

Figure 2: Wind speed estimate at RP 3000 based on the GCM ensemble mean. 9

2.4 Surface Roughness 9

Figure 3: Upwind Surface Roughness Conditions Required for Exposure B, sourced from ASCE7 Figure C26.7-1 10

Figure 4: Surface roughness examples for Miami-Dade county. 10

2.4 Historical Wind Data: Hurricanes, tornadoes, and other severe wind 11

2.4.1 Historic Hurricanes: 12

Figure 5: Example of a historical storm track (Hurricane Ida). 12

2.5 Wind Factor Scoring 13

WIND RISK METHODOLOGY **13**

3.1 Archetype Development 14

3.2 Risk Modeling 14

3.2.1 Damage simulation 14

Figure 1: Illustration of wind demand calculation for the 3D damage model. Left: residential building wall calculation. Right: commercial building roof calculation 15

Figure 2: Illustration of rain intrusion calculation following breach 16

3.2.2 Consequence Assessment 17

3.3 Loss Curves 17

Figure 4. Loss curves for a 1-story commercial building with a non-concrete roof in a high wind zone, high missile environment for the 10th, 50th, and 90th percentile losses. Loss from rain damage included. Left: downtime curve. Right: financial loss curve. 18

3.4 Key limitations 18

REFERENCES: **19**

APPENDIX: **21**

Climate Model Selection & Sensitivity 21

Table A1: Global Climate Models used in the FSF-WM 21

Figure A1: Average wind speed across all grid cells by GCM model 22

EXECUTIVE SUMMARY

Physical property damage from Tropical Cyclones has been rising in the United States, and is expected to continue rising in the future (A. Smith et al., 2022). Winds from hurricanes and tropical storms can cause significant damage to property and infrastructure and pose a serious threat to human life. Hurricane winds span large areas, reach high speeds, and are accompanied by heavy rainfall which can cause destructive flooding. In addition, hurricanes can cause widespread power outages and disrupt essential services, such as water and gas supplies. Notably, hurricanes affect communities within the United States more frequently and severely than other natural disasters (Cutter & Emrich, 2005). As a result, Tropical Cyclones have caused a total of $1.194 trillion (CPI adjusted) in losses in the United States between 1980 and 2022, with an average cost of approximately $21 billion per event. Additionally, the annual economic costs have increased each of the last four decades (A. Smith et al., 2022). Of the approximately $41-70 billion in losses due to Hurricane Ian in 2022, it is estimated that half of those damages ($23-35 billion) were due to wind damage (Core Logic, 2022). Given the increasing damage estimates from tropical cyclones, there is a need to evaluate the probable changes in wind exposure in the future in order to provide US residents an informed understanding of their risk .

The First Street Foundation Wind Model (FSF-WM) combines open data, open science, and engineering expertise to create a new Tropical Cyclone wind model that assesses hyper-local climate wind risk across the Nation, and can inform actions to address that risk. The FSF-WM uses high resolution topography, computer modeled hurricane tracks, and property data to create Tropical Cyclone wind hazard information for the contiguous United States, allowing a detailed evaluation of probable wind speeds by return period, and a comparison of this wind risk between the current year and 30 years in the future. When coupled with archetype-specific damage curves developed with the global engineering firm Arup, property level losses are also estimated. The hazard information provided by the FSF-WM relies on information from approximately 50,000 synthetic hurricane tracks, created by computer models and based on historical storms, to enable robust statistical sampling of hurricanes' characteristics (Emanuel et al., 2006). These synthetic tracks and their concomitant wind fields are downscaled using surface roughness corrections at the 30 meter resolution, for multiple return periods, and are projected 30 years into the future using the World Climate Research Programme (WCRP) Climate Model Intercomparison Project 6 (CMIP6) climate models (WCRP).

The FSF-WM reveals extensive risk along the Gulf and Southeastern Atlantic Coasts, with significant growing risk in the Mid-Atlantic and Northeastern regions of the country. Overall, in the next 30 years, the expected Average Annual Loss (AAL) resulting from this risk increases from $18.5 billion to $19.9 billion, and 13.4 million properties are likely to face Tropical Cyclone wind risk that do not currently face such risk. Most alarming is the economic risk in the state of Florida, where current levels of expected annual losses are already over 4 times the economic risk of the rest of the Gulf Coast combined, and account for approximately 73% of all expected damages nationally.

DATA SOURCES & TERMINOLOGY

The First Street Wind Risk product is based on a number of data sources (Table 1). We relied to the fullest extent possible on open datasets from the U.S. Federal government to encourage reproducibility and further research efforts in the field. These sources are augmented with local and commercial sources when required to complete the wind risk product.

Table 1: Data Sources

Name	Subject	Source	Notes
Hurricane Tracks		Rhodium Group & WindRiskTech LLC	
National Land Cover Database	Land cover	USGS	2019 Release
HAZUS	Surface roughness coefficients	FEMA	
HURDAT2	Historic Hurricanes	NOAA Atlantic Hurricane Center	
NOAA Storm Events Databases	Historic severe wind records, historic tornado records	NOAA	
Property Boundaries and characteristics	Descriptive information for properties	Lightbox	Aggregated from public records; Commercial but available
Building footprints	Building location on properties	Mapbox	Aggregated from satellite imagery and public records; Commercial but available

Abbreviations:

CMIP6 - Coupled Model Intercomparison Project version 6
GCM - Global Climate Models
CONUS - Contiguous United States
NOAA - National Oceanic and Atmospheric Administration
SPC - Storm Prediction Center
SSP - Shared Socioeconomic Pathway
USGS - U.S. Geological Survey

WIND HAZARD METHODOLOGY

The First Street Foundation Hurricane Wind Model (FSF-WM) combines open data, open science, and engineering expertise to create a new hurricane wind model that assesses hyper-local climate wind risk across the Nation, and can inform actions to address that risk. The FSF-WM uses high resolution land surface information, computer modeled hurricane tracks and property data for the contiguous United States to create wind hazard information for multiple return periods, a detailed evaluation of probable wind speeds and archetype-specific expected damages developed with the global engineering firm Arup, and a comparison of hurricane wind risk between the current year and 30 years in the future.

2.1 Hurricane Tracks

The FSF-WM uses large numbers (~10^4) of synthetic hurricane tracks derived under current (2015-2030) and future (2079-2099) CMIP6 defined climatic conditions. Hurricane tracks for the FSF-WM were provided by Rhodium Group and WindRiskTech LLC and generated using methods that have been described in detail in previous peer-reviewed publications and validated well against historical observations (Emanuel et al. 2004, 2006, 2013, 2015). We describe the methodology in brief below, but refer readers to the original publications for a more detailed description of the tropical cyclone downscaling model used for track generation.

The track generation process starts with a monthly representation of the mean thermodynamic conditions for a given climate state, defined with sea surface temperature and air temperature and humidity at all model levels up through the lower stratosphere from a GCM or reanalysis. Daily winds at the 250-hPA and 850-hPA levels are used to create synthetic time series of winds at both levels that are constrained to have the same monthly means, variances, and covariances as the global model, and a power spectra that falls off with the cube of the frequency. Weak protocyclonic disturbances are then introduced randomly in space and time and allowed to move according to the weighted mean of the 250- and 850-hPa flow and a correction for beta drift (Marks 1992). The hurricane intensity is integrated along each track via the Coupled Hurricane Intensity Prediction System (CHIPS), a highly resolved coupled ocean-atmosphere model solved in angular momentum coordinates (Emanuel et al. 2004). During this process, most of the protocyclonic disturbances die off and are discarded; the remaining disturbances that amplify to at least tropical storm intensity then define the tropical cyclone climatology of the given model.

Tracks from seven CMIP6 GCMs under scenario SSP245 were used in the FSF-WM (Table A1). The models selected include the GCMs that WindRiskTech has deemed adequate representations of the climate conditions necessary for studying tropical cyclone hazards. Consistent with other RiskFactor products, we use SSP245 as a middle of the road climate scenario that tracks well against current observations. For each GCM, 50 tracks per year that made landfall in the continental United States with least tropical storm intensity were generated for both the current (2015-2030) and end of century (2079-2099) scenarios. To more accurately characterize the tails of the hurricane intensity distribution, an additional 25 tracks per

GCM/year were generated using a higher intensity threshold. As a final layer of variance, every track was replicated into two additional ensemble members with slightly different storm characteristics. These included track paths that were jittered based on a statistically informed random walk of the original path and pressure and radii values that were randomly sampled from a lognormal distribution (Chavas and Emanuel, 2010). Combining all ensemble members resulted in 3600 and 4735 unique storms per GCM in the current/future periods, for a total universe of 58,345 unique hurricane tracks. An example subsample of a trackset is shown in Figure 1.

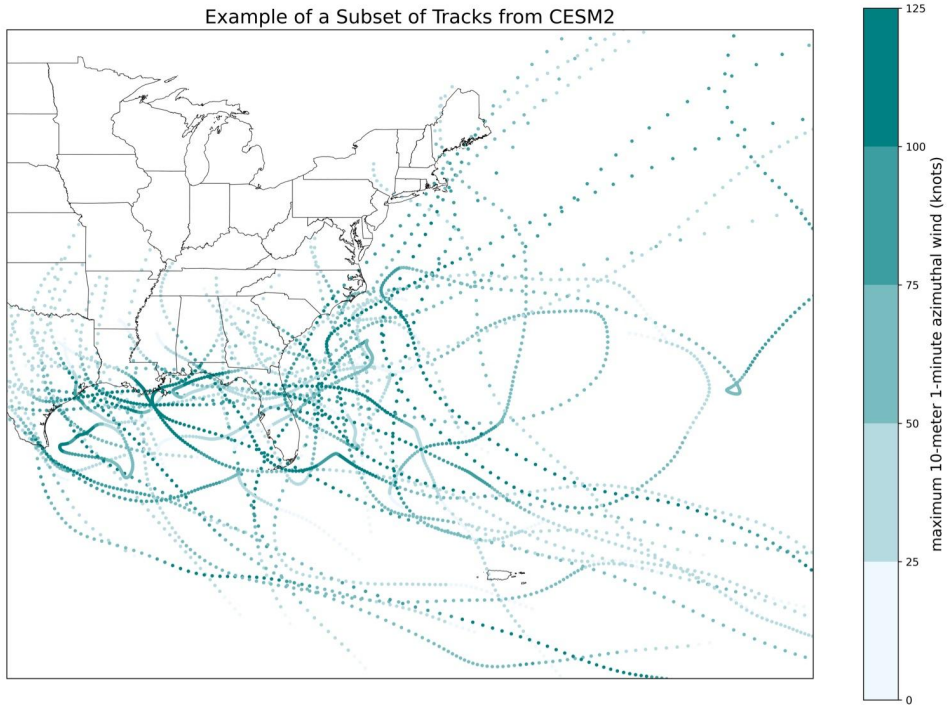

Figure 1: Sample of 50 hurricane tracks from the CESM2 Global Climate Model for the current time period (2015-2030).

2.2 Wind Field Modeling

In order to capture spatially heterogeneous wind velocities at specific locations, we used a combination of an axisymmetric gradient wind field model (Emanuel and Rotuno, 2011) and a boundary layer model (Vickery et al. 2009) to produce spatially continuous estimates of 10m sustained 1-minute wind fields for each synthetic hurricane track on fixed grid with 0.1 degree cell resolution. This process builds upon the pre-processed synthetic hurricane tracks described in section 2.1. All wind field modeling and calculations were performed using a set of MATLAB scripts originally provided by WindRiskTech and modified for application to the FSF-WM.

The wind field modeling workflow requires specification of one or more points of interest (POI) and a pre-processed synthetic track set. For the FSF-WM, fourteen unique GCM-timeframe combinations (7 GCMs under current and future conditions) were used. To define the area of

influence for the hurricane component of the FSF-WM, we ran the wind field modeling procedure for an initial set of POIs located at the centroids of 1.0 x 1.0 degree tiles across CONUS. Any tile that received tropical storm wind speeds or above in at least one hurricane track was subsequently split into 0.1 degree grid cells and included in the production POI list.

Given a POI and trackset, surface wind speeds were derived in the following steps. First, a radial profile of gradient wind from Emanuel and Rotuno (2011) is fitted to the model-predicted peak gradient wind speed and radius of maximum winds, including the effects of secondary eyewalls. This profile was then modified to account for storm translation and effects of environmental wind shear. The track set is then filtered to events that pass within 750 km of the point of interest at any point along their paths. This reduces the computational time needed for a given simulation by excluding tracks that do not produce winds at the POI. The wind speed and direction at the POI location is calculated at thirty minute time steps for each track using the wind field described above and the distance between the track and the POI. The wind speeds are converted into 1-minute sustained surface wind speeds at 10m height for each time step using surface drag coefficients. The surface drag coefficient data is natively stored at 25 km horizontal resolution and interpolated to the point of interest. This step accounts for the spindown of the hurricane vortices over cold land and the decay of surface winds over rough terrain.

The wind field workflow returns matrices of wind speed and direction for every storm in the event set. We generated 1-minute sustained wind estimates for all POIs across all fourteen hurricane track sets. For each scenario, the wind speed matrices were filtered to return the maximum surface wind speed for each track. The wind direction matrices were converted into frequency distribution tables showing the percentage of storms at the POI across eight cardinal directions in 45 degree bands. We restricted the direction calculations to only include storms reaching hurricane intensity (> 74mph).

2.2.1 Wind hazard statistics

To generate return period and frequency statistics for each POI, we start with Track IDs from sampling tables provided by the Rhodium Group that contain 1000 simulated time series of tropical cyclones in a given year (2015-2099) for each GCM and scenario. The sampling tables were constructed by randomly selecting Track IDs into a given yearly time series using the baseline hazard information associated with each track, then allowing each track to have an equal probability chance to randomly swap to either one of its ensemble members. For years in between the 2015-2030 and 2079-2099 tracksets, the sampling tables pull a linear combination of track IDs from both current and future track sets, with increasing contributions from end of century storms as the years increase. This process mixes the temporal pattern seen in sea level rise with the stable signals in GCM changes over the century. We focus on the 2015-2030 and 2045-2060 time periods for the FSF-WM.

For each grid cell, we draw the maximum surface wind speed corresponding to the Track IDs across all 1000 simulations in the sampling table and generate frequency counts in 10 mph bins

from 0 mph to 220 mph. These are converted annual exceedance probabilities under a Poisson distribution:

$$P(exceedance) = 1 - e^{-\mu t}$$

Where μ is the counting rate, and t is the time period of interest. These 10 mph binned values are interpolated with cubic splines to return the wind speeds corresponding to specific 2, 5, 20, 100, 300, 500, 700, 1700, 3000 year return periods. To account for year-to-year variability across the current and future scenarios, the statistics for each year within a given time window is weighted using the average number of landfalling storms across the synthetic time series relative to the entire population of storms. This process is repeated for the track sets from each GCM.

Due to variability in the climate conditions within the GCMs, the simulated hurricane tracks and resulting windfields show significant variation in location and magnitude across climate models, even after thousands of simulations (Table A1). As a general rule, for statistics in the FSF-WM, we use an ensemble mean with equal weights on all seven GCMs. For instances in lower return periods (2-year and 5-year) where less than seven models contain wind speed information at every POI, we ensemble average all available GCMs provided at least two are available.

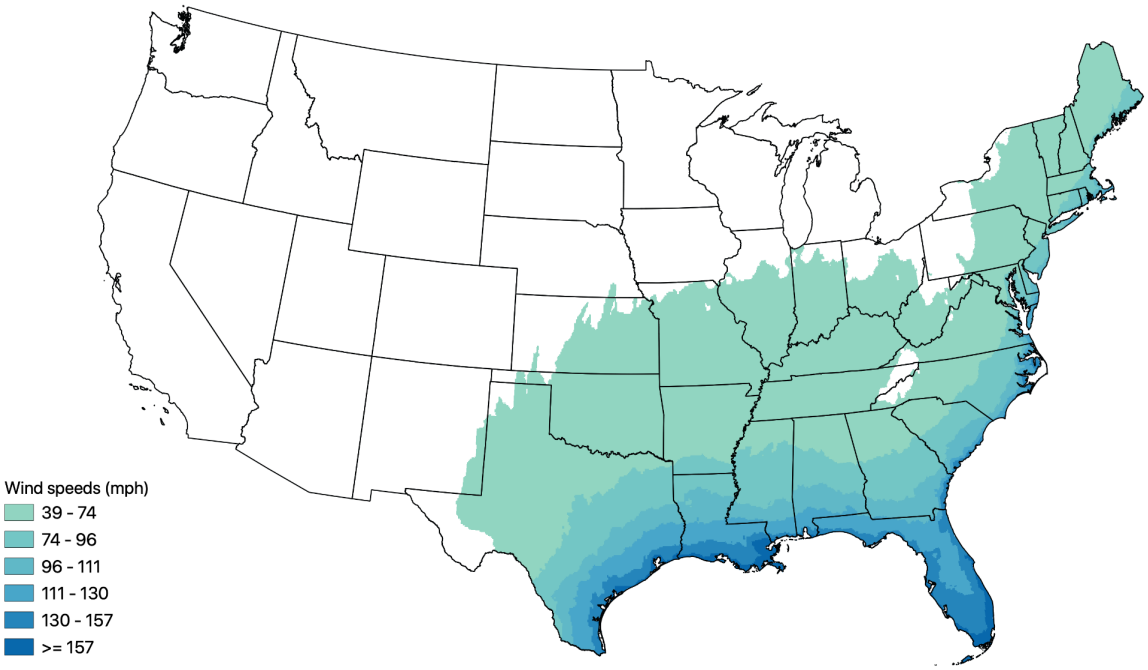

Figure 2: Wind speed estimate at RP 3000 based on the GCM ensemble mean.

2.4 Surface Roughness

The hurricane wind field model does not account for the hyper-local effects of surface roughness on wind speeds. Very rough areas, such as suburban or heavily forested areas, can decrease wind speeds, while open terrain can increase wind speeds. At the hyper-local scale, we implement a surface roughness correction to the hurricane wind field model output (1-minute sustained wind speeds and direction) with local terrain data.

2.4.1 Deriving surface roughness coefficients

We start with surface roughness length information (z0) at a 30-meter resolution, derived from the FEMA Hazus Hurricane Model (FEMA, 2021). A z0 value ranges from 0.003 meters (open water) to 1.5 meters (center of a tall city), and represents the effect of obstructions and vegetation on the shape of the boundary layer wind velocity profile. The z0 values from HAZUS (Tables 4-13 and 4-14) are segmented by land cover classifications within the U.S. Geological Survey National Land Cover Database (NLCD) and state or regional classifications. In states without z0 coefficients, we used the mean values per land cover class. To account for the separate regions in Florida and New York we used the county boundaries that most closely matched each region.

To model the potential effects of surrounding terrain on wind speeds, we calculate a moving average to represent the ground surface roughness around any given structure. We use exposure categories from the American Society for Civil Engineers (ASCE) guidelines for wind loads on building exposures to determine the averaging radius. We use the “Exposure B” calculations to determine the radii at which to take the moving averages, as Exposure B is defined as urban and suburban areas, wooded areas, or other terrain with numerous closely spaced obstructions having the size of single-family dwellings or larger. Additionally, it is estimated that the majority of buildings have an exposure category that is considered Exposure B (Ho 1992).

For Exposure B, the ground surface roughness values prevail for the following distances:

1. Buildings with a mean roof height of less than or equal to 30 ft = 1500 feet radius
2. Buildings with a mean roof height of greater than 30 ft = 2600 feet radius

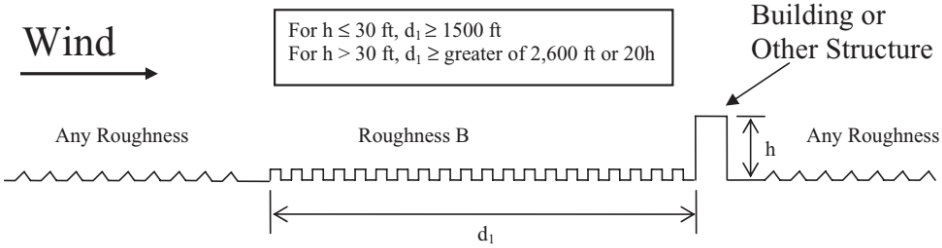

Figure 3: Upwind Surface Roughness Conditions Required for Exposure B, sourced from ASCE7 Figure C26.7-1

Based on this guidance, we create circular moving average raster layers from the 30-meter z0 values at both a 1,500 ft and 2,600 ft radius. We also create eight moving average rasters for both radii in 45 degree directional windows to account for how wind speeds may vary depending on the direction of approach.

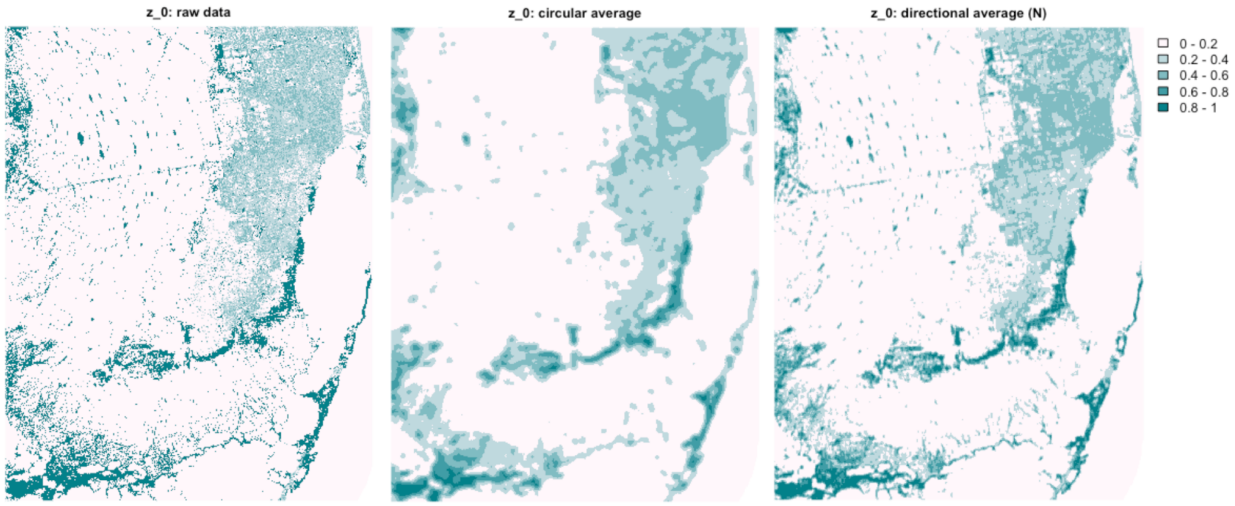

Figure 4: Surface roughness examples for Miami-Dade county.

2.4.1 Applying roughness coefficients to adjust wind speeds

For each property in the Lightbox database, roughness values for the gust derivation are extracted at the parcel centroid.

The final z0 values are then used to adjust the modeled wind speeds for local roughness effects. Wind speeds at different heights in the vertical wind profile are be extracted using the power law, which can be defined as:

$$\frac{v_z}{v_g} = \frac{z}{z_g}^{n} \text{ (Irwin 2006)}$$

Where, *v_z* represents the wind speed at height *z*, *v_g* represents the wind speed at height *z_g*, and *n* is the power law exponent related to the wind speeds at heights *z* and *z_g* that will incorporate surface roughness. The power law is then applied to the exposure coefficient (*k_z*) in ASCE7 as a factor that allows for the type and height of an exposure to be applied to gust loads. The equation for the exposure coefficient for any structure above 15 feet is defined as:

$$K_z = 2.01\left(\frac{z}{z_g}\right)^{2/\alpha} \text{ (ASCE7 Equation C27.3-1)}$$

Where, z is height of interest (10 meters), α is the wind shear exponent that depends on z0, and z_g is the gradient layer height. It can then be assumed that this equation implies that the wind velocity profiles can take the form of:

$$\frac{V_{gust}(z)}{V_{gust\ (basic)}} = \sqrt{2.01}\left(\frac{z}{z_g}\right)^{1/\alpha} \text{ (Irwin 2006)}$$

Where, z_g and α are defined as:

$$\alpha = c_1 z_o^{-0.133} \text{(ASCE7 Equation C27.3-3)}$$

Where, $c_1 = 5.56\ (when\ z_0\ and\ z_g\ are\ in\ meters)$

$$z_g = c_2 z_o^{0.125} \text{(ASCE7 Equation C27.3-4)}$$

Where, $c_2 = 450\ (when\ z_0\ and\ z_g\ are\ in\ meters)$

We assign each property a wind speed based on applying surface roughness coefficients for each direction to the speed produced by the model, then weighting based on the percentage of hurricane force winds from each direction. If a property has more than 75% of winds coming from a single direction, we instead use the circular average surface roughness to avoid the edge cases where only a few hurricane tracks contribute to the direction information.

The adjusted wind speeds are then converted from 1-minute sustained winds into a 3-second gust by averaging across the four gust factor curves presented in Vickery & Skerlj (2005). The gust factor for converting winds from 60 seconds to 3 seconds comes out to 1.28.

2.4 Historical Wind Data: Hurricanes, tornadoes, and other severe wind

The FSF-WM also includes historical data on hurricane events, tornadoes, and severe storm wind events, sourced from freely available government datasets that have varying levels of quality control. We present this information on an “as-is” basis, with minimal modeling applied only to ensure consistency in metrics across data layers. We provide basic information on each data layer below, referring readers to the original sources for more detailed background on each product (NOAA 2022, n.d.).

2.4.1 Historic Hurricanes:

Historical cyclone data was sourced from the NOAA National Hurricane Center Atlantic hurricane database best track data (HURDAT2) (NOAA, n.d.). HURDAT2 data includes 6-hourly data on the location, maximum winds, and central pressure of historic cyclone events from 1851-2021. The size of historic cyclones, including radii for 34, 50, and 60 knot winds and the radius of maximum winds, are provided from 2004-2021. For pre-2004 events, we assume the size of the cyclone based on the Saffir-Simpson scale and the average radii across similar category storms in the post-2004 events to determine counties that were likely affected by the storm path. For post-2004 events, The provided radii extents in the northeastern, southeastern, southwestern, and northwestern directions were used to create a buffer around each measurement, which were then interpolated to create continuous regions of maximum wind for each storm track. We apply the gust-conversion factor (1.28) derived for the hurricane wind model to estimate the 3 second gusts associated with each historical storm. We note that these gust estimates are simplistic approximations based on coarse data and may vary from observed gusts recorded at specific locations.

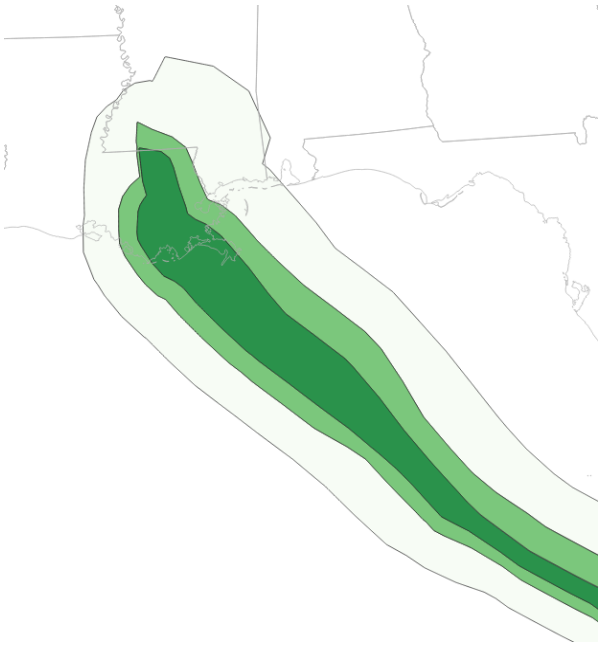

Figure 5: Example of a historical storm track (Hurricane Ida).

2.4.2 Tornadoes

Historical tornado information was sourced from the NOAA Storm Prediction Center's Severe Weather Database (NOAA, 2022). Individual tornado entries exist from 1950 through 2021. The tornado information includes the intensity of each event, which is measured on the Fujita Scale until 2007 and the Enhanced Fujita scale after 2007, as well as information on injuries, fatalities, and economic losses in U.S. dollars. Individual events are stored as either points or linestrings, which we aggregate to counties based on intersections with the county boundaries. We define 'affected counties' with summary statistics including storm count, injuries, fatalities, and losses. We do not account for specific tornado outbreaks or other clustering of storms.

2.4.3 Other Severe Wind

Other severe wind data (mostly thunderstorms) were also sourced from the Severe Weather Database (NOAA, 2022). Wind events are represented in the database from 1955 through 2021. The majority of reports are verified by falling trees or damage to buildings, not by observed wind gusts. This means that there is a possible bias towards areas with trees or higher population density. Individual entries for events in the database can include multiple reports of damage or injury for a particular weather event, so data points are aggregated both by geography (county) and temporal proximity. A series of events within a county where an event occurred within three hours of the next event are considered a cluster. Wind event intensities are reported as maximum wind speed (where available) instead of a categorization.

2.5 Wind Factor Scoring

Consistent with other Risk Factor products, every residential and commercial property across the United States is assigned a Wind Factor score ranging from one to ten that reflects the hazard exposure at the property. For Wind Factor, the averaged wind speeds across return periods are used to determine the score at each property. First a raw score is computed, which is an expected value based on the speed (*s*) by return period (*r*), with only winds of tropical-storm-force or better are considered:

$$\sum_{n} \frac{s_i + s_{i+1}}{2(r_{i+1} - r_i)}$$

In other words, for return periods with speeds below 39 mph, *s* is zero. Winds with speeds less than tropical storm are excluded on the basis that they do not produce damage to structures.

This raw score is computed for both current (2023) and future (2053) conditions and averaged, then partitioned into ten bins that reflect the internal probability distribution. The first bin, minimal risk, is reserved for properties that do not experience winds of tropical storm force in any of the modeled return periods. The top bin, extreme risk, reflects risk of a tropical storm in return period 2 and all less common probabilities.

WIND RISK METHODOLOGY

ARUP

The documentation sections for the hurricane wind risk calculations were provided by Arup.

The risk modeling approach simulates the impact of hundreds or thousands of different hurricane scenarios using a virtual model of the building to estimate the extent and severity of hurricane damage on individual building components and translates it to consequences such as financial loss and downtime. Following the risk modeling approach, a series of curves reflecting downtime and financial loss from wind events were developed for a suite of building archetypes. A rigorous simulation-based methodology was used to develop these curves. The following discusses how the archetypes were determined and the methodology for developing the curves.

3.1 Archetype Development

A set of 30 non-residential and 26 residential archetypes were developed and selected for assessment. The following key building characteristics were considered: Building occupancy (e.g., industrial, commercial, residential), number of stories, roof material (concrete topping or non-concrete topping roof), missile environment (high or low), and design wind speed zone (this determines the envelope component wind resistance). These are the most critical building characteristics that will affect both building performance during damaging wind events as well as the associated financial loss and downtime (FEMA, 2000). These characteristics are also selected based on the availability of First Street Foundation building data inventory. Based on

the building inventory data First Street Foundation provided, the range of each characteristic was selected to best cover the building stock data. The archetypes were developed considering the practical and possible combinations of these different characteristics.

3.2 Risk Modeling

The risk modeling approach simulates the impact of wind scenarios using a virtual model of the building to estimate the extent and severity of wind damage on individual building components and translates it to consequences such as financial loss and downtime. Arup developed this component-based approach for wind risk analysis based on a methodology that was originally used to quantify seismic risk, adopted from FEMA P-58 (Applied Technology Council, 2013) and enhanced to more realistically capture building downtime with Arup's Resilience-based Earthquake Design Initiative (REDi) methodology (Arup, 2013). In the past several years, Arup has adapted this seismic component-level approach to climate-related hazards.

3.2.1 Damage simulation

General approach

The building models were populated with typical building components that could be damaged in wind events. During an actual wind event, how a given building component is impacted depends on the location of the component, the orientation of the component, the interaction with other components, the wind resisting capacity of the component, etc. These complexities were explicitly captured by creating a 3D physical based simulation model for each building archetype. The simulation procedure developed captures the following key features:

- Component location, orientation, and the geometry effect of wind pressure
- Progressive failure behavior of components and interaction between components
- Updates to the internal pressure due to envelope component breach
- Wind-driven rain damage due to envelope breach
- Uncertainty of wind pressures and wind resisting capacities

The general procedure considered for damage simulation is consistent with the state-of-art methods in the field (FEMA 2000, FPHLM 2015, Abdelhady et al. 2021, Alduse et al. 2022).

3D wind damage simulation model

For each building archetype, the envelope building components are included explicitly in a 3D model. For each wind event simulated, the pressure load on each individual component was calculated based on the wind direction, component geometry, location, and other characteristics. The pressure load on each component was compared with the component's wind resistance. Failure was determined when the pressure load/uplift force on one unit is larger than the capacity of the associated failure mechanism. Figure 1 shows an example of a damage assessment for a typical residential wall component and typical commercial roof component. This process was conducted for each component unit modeled for each archetype.

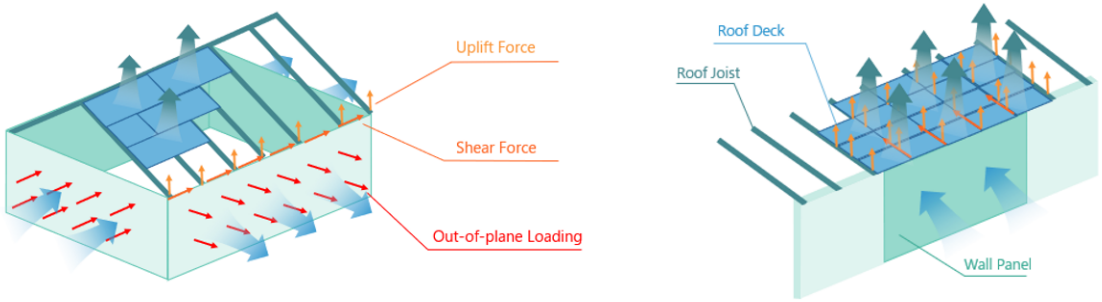

Figure 1: Illustration of wind demand calculation for the 3D damage model. Left: residential building wall calculation. Right: commercial building roof calculation

For all archetypes other than single family residential buildings, the envelope components included were windows, doors, roller doors, roof cover, roof deck, roof joist, wall panels, rooftop equipment (e.g., cooling equipment for the HVAC system), and exterior ground equipment (e.g., transformers). Note that not all components were included in the model for every archetype. For the single-family house archetypes, the building envelope components included were windows, doors, garage doors, roof cover, roof sheathing, roof trusses, and wall panels. Each unit of the component type is assigned in a 3D building geometry model based on assumed distribution and quantity.

Wind pressure calculation

The wind pressure is calculated based on the wind speed, wind direction and the wind pressure coefficients following general procedures described in ASCE 7-22 (ASCE 22). The external pressure coefficients are a function of the location of the component unit and the direction of the wind. For each individual component unit considered in the 3D model, the location zone was assigned. The corresponding pressure coefficient for the location zone was selected for the calculation. These pressure coefficients were obtained from Banik et al. (2017), which were derived from past wind tunnel tests.

Wind resisting capacity

The wind resisting capacity for each failure mechanism for each component is explicitly assigned for each archetype. For non-single-family archetypes, it is assumed that the components are designed to fulfill code requirements based on the design wind speed, and the capacity of each component was calculated accordingly. Three levels of building component capacities were considered for different archetypes (100 mph, 125 mph, and 160 mph design wind speed for low, medium, and high wind zones, respectively). For single family archetypes, the component capacities are determined based on available literature data (FEMA 2000, FLPHM 2015). The capacity is also updated dynamically through the simulation. For example, when a given connection fails, the capacity will be reduced for the adjacent component.

Rain intrusion damage

During a hurricane event, rain intrusion could occur through the damaged envelope components. 24-hour rainfall amounts were obtained based on the relation developed by Pita et al. (2012). The amount of rain entering each floor is explicitly calculated based on the breach area of the roof and/or side envelope of the building. The interior damage percentage was estimated based on the water depth following the relation in Hazus (FEMA 2000). The interior damage percentage was used in the consequence calculation to estimate the cost and downtime due to interior rain damage.

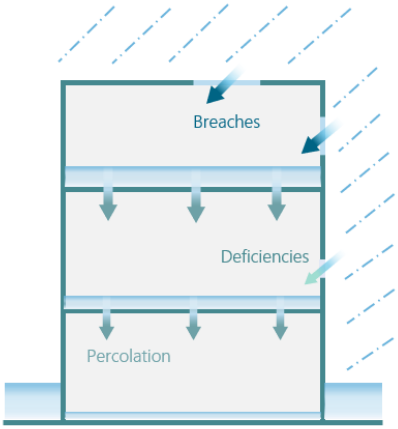

Figure 2: Illustration of rain intrusion calculation following breach

Treatment of uncertainty

To account for the uncertainty involved in the simulation process, the damage simulation for each wind event was repeated 500 times. A Monte Carlo simulation procedure was used to sample the capacity for each individual component unit from the predefined distributions and to account for the uncertainty in the components wind resistant capacities. The wind pressure coefficient on each component was also sampled for each realization. Note the sampling was conducted independently for each individual component unit assessment. The distribution parameters used followed the recommendation in Vickery et al. (2006).

3.2.2 Consequence Assessment

Each building archetype was subjected to wind speeds ranging from 30 mph to 200 mph in 10 mph increments and 8 different wind directions. For each wind speed and direction, 500 Monte Carlo simulations were run. Detailed component damage results were produced based on the damage simulation procedure discussed above for each of the 500 realizations. From the damage results, the number of units for each component needing to be repaired or replaced (according to its damage state) were obtained. This information was used for the financial loss and downtime calculations. Arup also developed consequence functions that link each component damage state to specific levels of financial loss and lengths of repair times. Based on the damage results, the consequence assessment was conducted to obtain the financial loss and downtime.

Financial loss

Financial loss values (i.e., the cost to repair or replace a component) were based on data procured by Arup's cost estimators. These costs were estimated for Washington, DC in 2022 USD. To get accurate financial loss estimates for other regions, First Street Foundation scales the financial losses using an appropriate metro area location factor from regional price parity data from the Bureau of Economic Analysis. Based on the level of damage, the total building financial loss was calculated for each realization as a sum across all damaged components. Financial loss values are reported as average loss per square foot.

Downtime

The downtime calculation followed the REDi methodology, which was originally published in REDi for Seismic (Arup, 2013) and adapted for wind by Arup. Downtime consists of repair times for damaged components and impeding factors that delay the initiation of building repairs. Impeding delays include time for returning from evacuation, building restoration, contractor and engineer mobilization, and equipment long lead times. Once the impeding delays are resolved, the downtime model allocates crews of workers to make repairs to damaged components based on specific trades (e.g., structural or building envelope). A construction of realistic repair sequences that mimic actual contractor logistics is aggregated to quantify the overall building downtime

3.3 Loss Curves

Once the downtime and financial loss have been calculated for each realization and for each wind speed and wind direction, a set of loss curves (financial loss vs wind speed, downtime vs wind speed) for all archetypes were calculated and provided to First Street Foundation. Downtime and financial loss curves, representing the 10^{th}, 50^{th} (median), and 90^{th} percentiles of the results were calculated.

Where possible, the loss ratios were compared against the Hazus hurricane model for similar archetypes as a benchmarking exercise (FEMA 2000). There was general agreement between Hazus and the models developed in this study on the wind speed thresholds where a significant increase in the building loss ratio is observed. Note that the archetype definitions, the damage and consequence modeling assumptions are different compared to Hazus, so the benchmark aims to seek agreement on the rough range of wind speeds observed.

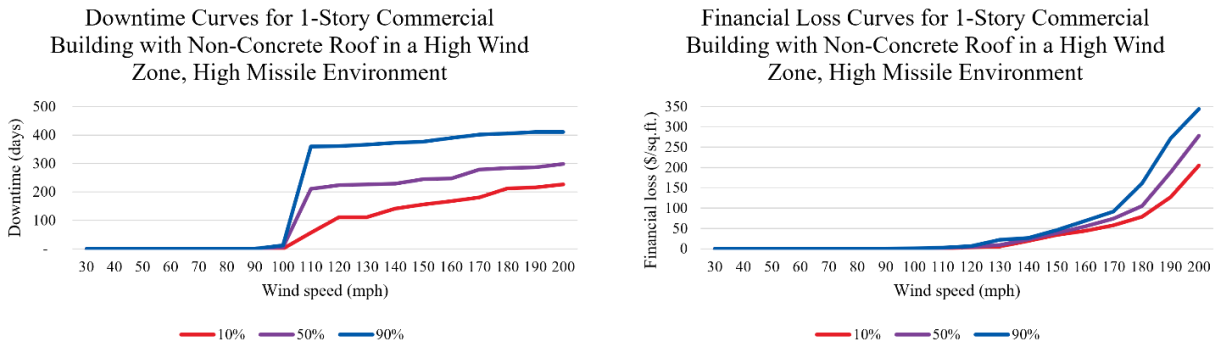

Figure 4. Loss curves for a 1-story commercial building with a non-concrete roof in a high wind zone, high missile environment for the 10th, 50th, and 90th percentile losses. Loss from rain damage included. Left: downtime curve. Right: financial loss curve.

3.4 Key limitations

- The wind archetype development assumes certain simplified building geometry, component type, number, location, roof construction type, etc. It might not perfectly represent the individual building in practice
- The component wind-resisting capacities vary significantly based on component condition, manufacturer, construction quality, local requirements. etc. No consistent wind-resisting data is available to date. The archetype considers generic wind zones to determine the wind-resisting capacity based on the design wind speeds. To capture the possible variability, the uncertainty of component capacities was explicitly considered by conducting Monte Carlo simulations. This is consistent with the state-of-the-art approach in wind risk assessment (FEMA 2000, FPHLM 2015, Abdelhady et al. 2021, Alduse et al. 2022)
- The tall building archetype development assumes a simplified wind profile along the building height based on ASCE 7 (ASCE 2022). Wind pressure on tall building components is complex due to local wind effect and dynamic wind effect. Wind tunnel tests or CFD are often needed. Given the general purpose of the study, simplification has been used. Therefore, wind damage and associated consequence results for buildings more than 10 stories tall could be less accurate.
- As only a handful of archetypes were developed to represent the entire building stock, there are simplifications considered in mapping the archetype to represent each building given the building characteristics data available. The individual building characteristics might not be sufficiently captured by the assigned archetype.
- The rule of mapping the individual asset to building archetype is developed to cover generic cases. The rule might not apply to individual building with special characteristics.

REFERENCES:

Abdelhady, A. U., Spence, S. M. J., and McCormick, J. (2021). "A Resilience-Based Assessment of the Performance of Residential Communities Subject to Hurricane Hazard." *Proceedings of International Structural Engineering and Construction*, 8(1), doi: 10.14455/ISEC.2021.8(1).RAD-09.

Alduse, B., Pang, W., Tadinada, S.K., and S. Khan. (2022). "A Framework to Model the Wind-Induced Losses in Buildings during Hurricanes." *Wind*, 2(1), 87–112, doi: 10.3390/wind2010006.

American Society of Civil Engineers (ASCE). (2022). *Minimum Design Loads for Buildings and Other Structures. ASCE Standard ASCE/SEI 7-22*. American Society of Civil Engineer, Reston, US.

Applied Technology Council. (2013). *FEMA P-58 Seismic Performance Assessment of Buildings Volume 1 - Methodology.* Retrieved from https://femap58.atcouncil.org/documents/fema-p-58/24-fema-p-58-volume-1-methodology-second-edition/file

Arup. (2013). *REDi Rating System: Resilience-Based Earthquake Design Initiative for the Next Generation of Buildings.* Retrieved from https://www.arup.com/perspectives/publications/research/section/redi-rating-system

Banik, S., Twisdale, L., Vickery, P., and Quayyum, S. (2017). "Progressive failure of building cladding in high winds." *PSA2017*, Pittsburgh, PA, September 24-28, 2017.

Chavas, D. R., and Emanuel, K. A. (2010), A QuikSCAT climatology of tropical cyclone size, *Geophys. Res. Lett.*, 37, L18816, doi:10.1029/2010GL044558.

Emanuel, K., C. DesAutels, C. Holloway, and R. Korty, (2004): Environmental control of tropical cyclone intensity. J. Atmos. Sci., 61, 843-858.

Emanuel, K., (2006): Climate and tropical cyclone activity: A new model downscaling approach. *J. Climate,* **19,** 4797-4802.

Emanuel, K., S. A. Ravela, E. A. Vivant and C.A. Risi, (2006): A Statistical-Deterministic Approach to Hurricane Risk Assessment. *Bull. Amer. Meteor. Soc.,* **87,** 299-314

Emanuel, K., (2011): Global warming effects on U.S. hurricane damage. *Wea. Clim. Soc.,*, **3**, 261-268.

Emanuel, K., & Rotunno, R. (2011). Self-Stratification of Tropical Cyclone Outflow. Part I: Implications for Storm Structure, *Journal of the Atmospheric Sciences*, *68*(10), 2236-2249.

Emanuel, K.A., (2013): Downscaling CMIP5 climate models shows increased tropical cyclone activity over the 21st century. *Proc. Nat. Acad. Sci.*, **110**, doi/10.1073/pnas.1301293110.

Federal Emergency Management Agency (FEMA). (2000). *Multi-hazard Loss Estimation Methodology-Hurricane Model.* Federal Emergency Management Agency, Washington, DC.

Federal Emergency Management Agency (FEMA), (2021). HAZUS Hurricane Model Technical Manual, HAZUS 5.1. Available at: https://www.fema.gov/sites/default/files/documents/fema_hazus-hurricane-model-technical-manual-5-1.pdf

Florida Public Hurricane Loss Model (FPHLM). (2015). *Florida Public Hurricane Loss Model 6.0.* Florida International University, Miami, FL.

Ho, E. (1992). "Variability of low building wind lands." Doctoral Dissertation,University of Western Ontario, London, Ontario, Canada.

Irwin, P. A. (2006). "Exposure categories and transitions for design wind loads." J. Struct. Engrg., 132(11), 1755–1763.

Irwin, J. S., (1979): A theoretical variation of the wind profile power law exponent as a function of surface roughness and stability. *Atmos. Environ.,***13,** 191–194.

Landsea, C. W. and J. L. Franklin, (2013): Atlantic Hurricane Database Uncertainty and Presentation of a New Database Format. Mon. Wea. Rev., 141, 3576-3592.

NOAA (2022). Storm Prediction Center GIS Page. Available at: https://www.spc.noaa.gov/gis/svrgis/

NOAA (n.d.). National Hurricane Center Data Archive. Available at: https://www.nhc.noaa.gov/data/

Pita, G., Pinelli J.P, Cocke, S., Gurley, K., Mitrani-Reiser, J., Weekes, J., and Hamid, S. (2012). "Assessment of hurricane-induced internal damage to low-rise buildings in the Florida Public Hurricane Loss Model." *Journal of Wind Engineering and Industrial Aerodynamics*, 104–106, 76–87, doi: 10.1016/j.jweia.2012.03.023

Vickery, P.J., and Skerlj, P.F. (2005) Hurricane Gust Factors Revisited, *Journal of Structural Engineering, 131(5),* 825-832.

Vickery, P., Skerlj, P., Lin, J., Tisdale, Jr., L., Young, M., and Lavelle, F. (2006). "HAZUS-MH Hurricane model methodology. II: Damage and Loss Estimation." *Natural Hazards Review*, 7(2), 94-103.

Vickery, P. J., Wadhera, D., Powell, M. D., & Chen, Y. (2009). A Hurricane Boundary Layer and Wind Field Model for Use in Engineering Applications, *Journal of Applied Meteorology and Climatology*, *48*(2), 381-405.

APPENDIX:

Climate Model Selection & Sensitivity

Table A1: Global Climate Models used in the FSF-WM

Model Name:	**Model Origin:**	**Model Agency:**
MPI6	Germany	Max Planck Institute
MRI6	Japan	Meteorological Research Institute, Japan
MIROC6	Japan	Atmosphere and Ocean Research Institute (The University of Tokyo), National Institute for Environmental Studies,and Japan Agency for Marine-Earth Science and Technology
ECEARTH	Europe	EC-Earth Consortium
UKMO6	United Kingdom	Hadley Centre for Climate Prediction and Research
NORESM6	Norway	NorESM Climate modeling Consortium (NCC)
CESM2	USA	National Center for Atmospheric Research (NCAR)

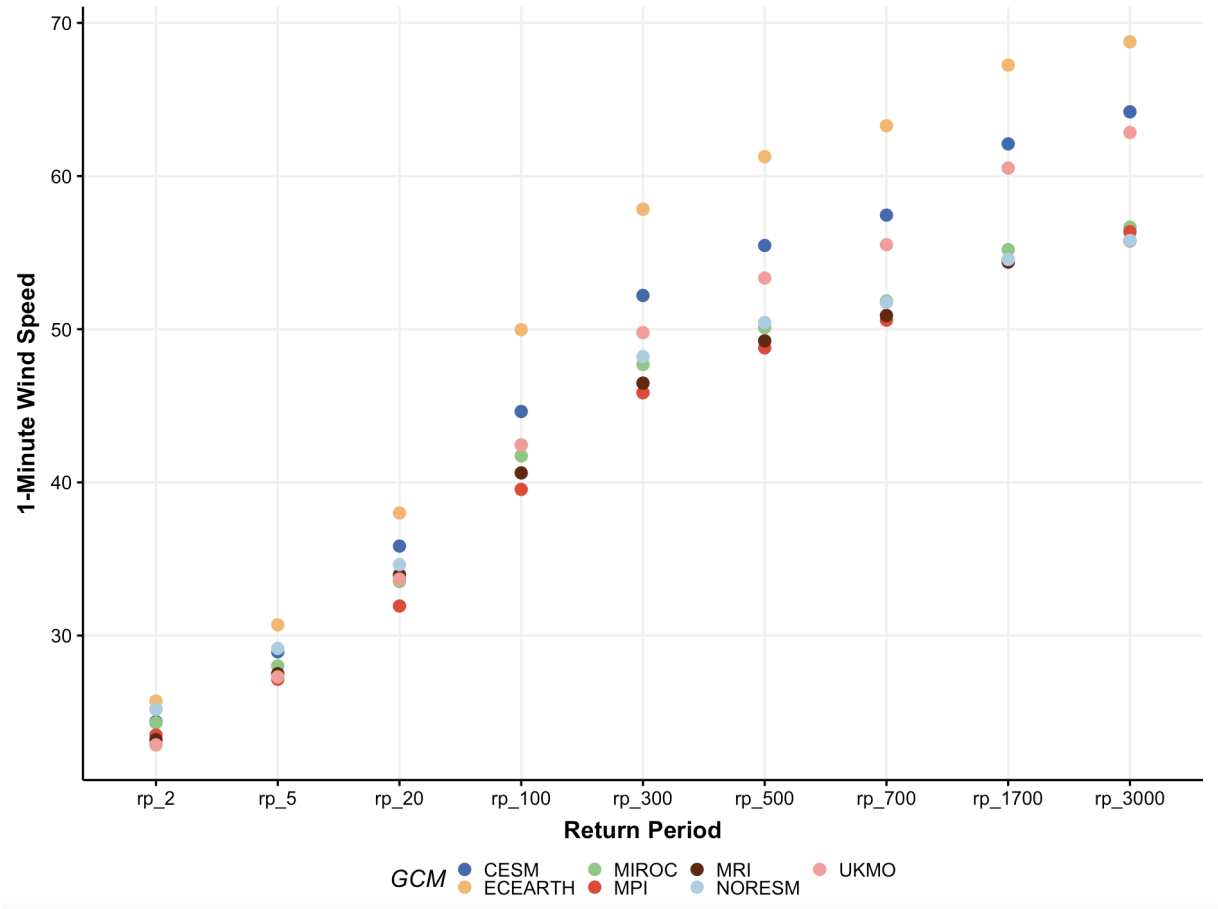

Figure A1: Average wind speed across all grid cells by GCM model